

Interacting Electron Wave Packet Dynamics in a Two-Dimensional Nanochannel

Christoph M. Puetter,^{1,2,*} Satoru Konabe,^{1,2} Yasuhiro Hatsugai,^{1,2,3} Kenji Ohmori,^{1,2} and Kenji Shiraiishi^{1,2,4}

¹*Graduate School of Pure and Applied Sciences, University of Tsukuba, 1-1-1 Tennodai, Tsukuba, 305-8577, Japan*

²*CREST, Japan Science and Technology Agency, 7 Gobancho, Chiyoda, Tokyo 102-0075, Japan*

³*Center for Interdisciplinary Research, Tohoku University, Sendai 980-8578, Japan*

⁴*Center for Computational Sciences, University of Tsukuba, 1-1-1 Tennodai, Tsukuba, 305-8577, Japan*

Classical and quantum dynamics are important limits for the understanding of the transport characteristics of interacting electrons in nanodevices. Here, we apply an intermediate semiclassical approach to investigate the dynamics of two interacting electrons in a planar nanochannel as a function of Coulomb repulsion and electric field. We find that charge is mostly redistributed to the channel edges and that an electric field enhances the particle-like character of electrons. These results may have significant implications for the design and study of future nanodevices.

Ideal ultrasmall logic nanodevices feature high switching speeds, low power consumption, excellent on-off current ratios and high scalability and integrability. Electron transport in ultrasmall nanodevices approaching channel lengths of approximately 10 nm, [1] however, turns out to be quasi-ballistic and intricate [2, 3] due to Brownian motion (thermal noise caused by scattering and diffusion) and the discreteness of the electric charge (leading to shot noise enhanced by unscreened trapped charges). These effects give rise to significant current fluctuations at high clock speeds and low voltages, [4, 5] which are detrimental to efficient device operation. This indicates that high-speed electrons in nanoscale regions cannot be described by conventional statistical frameworks such as Maxwell-Boltzmann approaches. Highly doped drain and source regions can further impact channel electrons, e.g., due to the build-up of mirror charges, suggesting that Coulomb interaction is a paramount ingredient in describing transport, dissipation, and equilibration in nanostructures. [2, 3, 6] A comprehensive understanding of electron dynamics on small time and length scales therefore is desirable to improve the device performance.

Various approaches to electron transport in nanodevices have been taken so far, ranging from classical Monte Carlo and molecular dynamics methods to quantum nonequilibrium Green function calculations. [2, 4, 5, 7, 8] Here, we address the charge transport from an intermediate, semiclassical perspective, [9, 10] by solving the Schrödinger equation numerically for a pair of interacting electron wave packets that propagate in a planar nanochannel. This approach interpolates between the classical, particle-like and the quantum, wavelike nature of electrons (Fig. 1) and approximately preserves the discreteness of the transported electron charge over appropriate (not too short) time scales. Wave packet approaches have been considered previously, but relied on strictly one-dimensional structures and/or on noninteracting electrons, or were based on approximate schemes such as the time-dependent Hartree-Fock theory. [11–17]

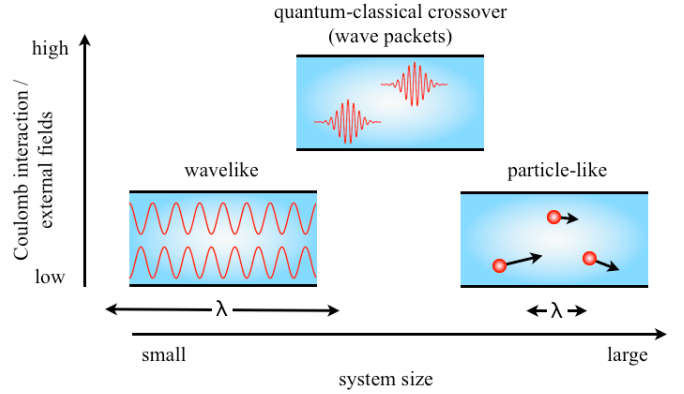


FIG. 1. Schematic illustration of classical (particle-based), quantum (wave-based) and intermediate electronic transport regimes applicable to a nanochannel. For intermediate system sizes a semiclassical approach based on a wave packet picture may be used, which is further strengthened by an external field and/or Coulomb interaction. (λ indicates the electron mean free path.)

Below, we study in detail the effect of Coulomb repulsion and an external electric field on wave packet propagation in a two-dimensional nanochannel. A main finding is that Coulomb repulsion redistributes the charge density to the channel walls, which makes electron transport more sensitive to perturbations at the interface. The presence of a uniform electric field, mimicking a channel potential, furthermore has a stabilizing effect on the wave packets, reducing the spreading along the channel direction and, hence, backing the more localized, classical particle-like picture often used in full-scale device simulations.

In order to study the propagation of two interacting electrons in a nanochannel, we solve the time-dependent Schrödinger equation $i\hbar\partial_\tau|\psi(\tau)\rangle = H(\tau)|\psi(\tau)\rangle$ numerically using a split-operator (Suzuki-Trotter) approach. [18–20] The total Hamiltonian $H(\tau) = H_{\text{kin}}(\tau) + H_{\text{int}}$

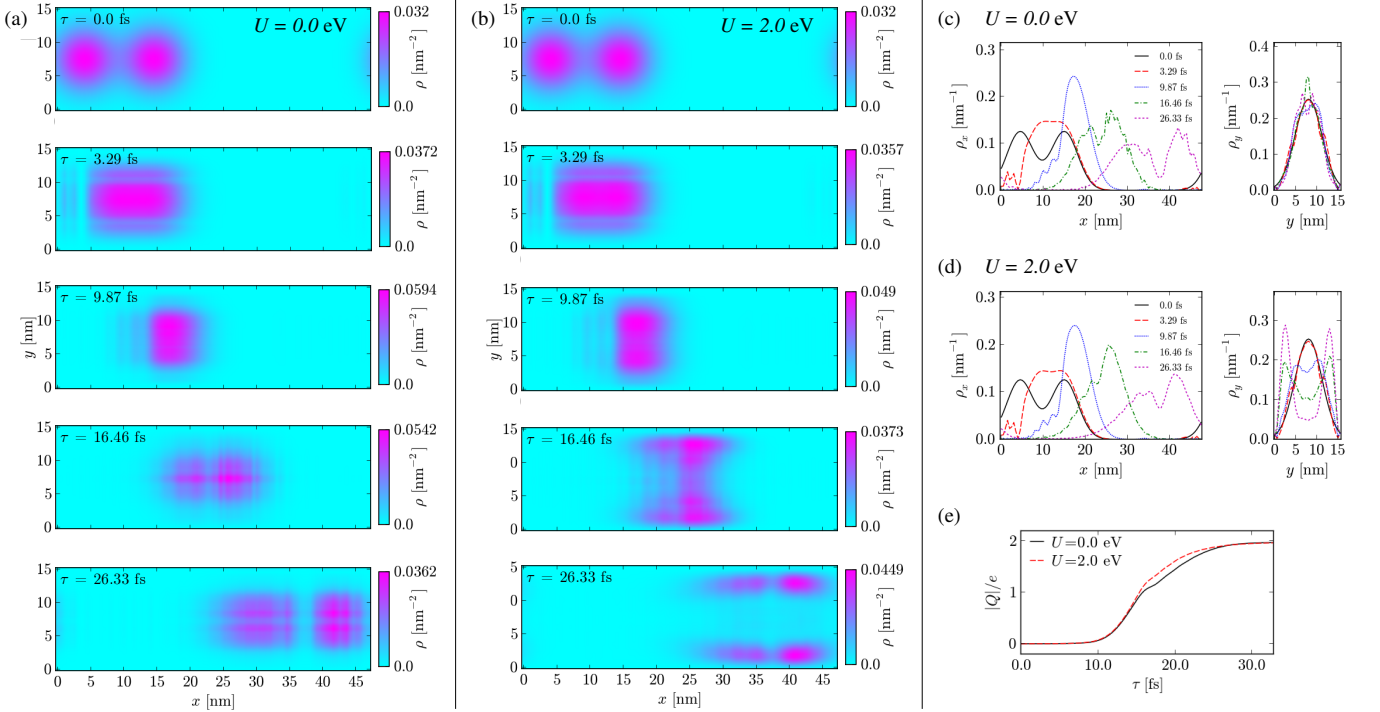


FIG. 2. Comparison of the time evolution of two noninteracting and two interacting electron wave packets in a two-dimensional nanochannel in the presence of an electric field applied in x-direction. (a), (b) Snapshots of the electron density $\rho(\mathbf{r}; \tau)$ for $U = 0$ and 2.0 eV, respectively. (c), (d) Corresponding partially integrated one-dimensional electron densities $\rho_x(x; \tau)$ and $\rho_y(y; \tau)$ for $U = 0$ and 2.0 eV, respectively. (e) Total charge transported across the half-way line at $x_0 = 23.5$ nm as a function of time τ . The initial sizes of the Gaussian wave packets are $\sigma_\tau = 9a = 4.5$ nm, and the electric field amounts to $E = 0.4$ MV/cm; only the incoming, initially left-hand side wave packet possesses initially a finite momentum $\mathbf{k} = (0.3\pi/a, 0)$.

includes a kinetic and a Coulomb interaction term, i.e.,

$$H_{\text{kin}}(\tau) = -t \sum_{\mathbf{r}} (e^{-\frac{i\epsilon}{\hbar} E a \tau} c_{\mathbf{r}}^\dagger c_{\mathbf{r}+\mathbf{a}_x} + c_{\mathbf{r}}^\dagger c_{\mathbf{r}+\mathbf{a}_y} + \text{h.c.}) \quad (1)$$

$$H_{\text{int}} = \frac{1}{2} \sum_{\mathbf{r}, \mathbf{r}'} \frac{U}{|\mathbf{r} - \mathbf{r}'|/a} c_{\mathbf{r}}^\dagger c_{\mathbf{r}} c_{\mathbf{r}'}^\dagger c_{\mathbf{r}'}, \quad (2)$$

respectively, where $c_{\mathbf{r}}^\dagger$ ($c_{\mathbf{r}}$) creates (annihilates) a spinless electron at site \mathbf{r} . Here, the kinetic Hamiltonian $H_{\text{kin}}(\tau)$ describes nearest-neighbor hopping processes with hopping amplitude t and is time-dependent through a Peierls phase factor to account for a uniform electric field $\mathbf{E} = (E, 0)$ in x-direction. By coupling the electrons to an electric field in this way, the channel potential along the x-direction can be modelled without spurious discontinuities along x associated with the finite size of a periodic channel (at the expense of the conservation of total energy), whereas closed boundary conditions are imposed along y. The lattice spacing and two lattice vectors of the underlying square lattice are denoted by a , \mathbf{a}_x and \mathbf{a}_y , respectively. The term H_{int} represents the long-range Coulomb interaction with interaction strength U .

We are interested in the evolution of the two-particle state $|\psi(\tau)\rangle = (1/\sqrt{2}) \sum_{\mathbf{r}, \mathbf{r}'} \Psi(\mathbf{r}, \mathbf{r}'; \tau) c_{\mathbf{r}}^\dagger c_{\mathbf{r}'}^\dagger |0\rangle$, where $\Psi(\mathbf{r}, \mathbf{r}'; \tau)$ stands for the antisymmetric two-particle real space wave function at time τ , normalized to

$\sum_{\mathbf{r}, \mathbf{r}'} |\Psi(\mathbf{r}, \mathbf{r}'; \tau)|^2 = 1$. With $L_x a$ and $L_y a$ denoting the extend of the lattice in x and y direction, the periodic and closed boundary conditions take the form $\Psi(\mathbf{r}, \mathbf{r}'; \tau) = \Psi(\mathbf{r} \pm L_x \mathbf{a}_x, \mathbf{r}'; \tau) = \Psi(\mathbf{r}, \mathbf{r}' \pm L_x \mathbf{a}_x; \tau) = \Psi(\mathbf{r} \pm L_x \mathbf{a}_x, \mathbf{r}' \pm L_x \mathbf{a}_x; \tau)$ and $\Psi(\mathbf{r}, \mathbf{r}'; \tau) = 0$ if $r_y, r'_y \geq L_y a$ or < 0 [$\mathbf{r} = (r_x, r_y)$, $\mathbf{r}' = (r'_x, r'_y)$], respectively. As an initial condition, we model the probability distribution of the electrons by two (moving) Gaussian wave packets centered at \mathbf{R} and \mathbf{R}' with momenta \mathbf{k} and \mathbf{k}' and width σ_τ ,

$$\Psi(\mathbf{r}, \mathbf{r}'; 0) = \frac{1}{\mathcal{N}} [\Phi_{\mathbf{k}}(\mathbf{r} - \mathbf{R}) \Phi_{\mathbf{k}'}(\mathbf{r}' - \mathbf{R}') - \Phi_{\mathbf{k}'}(\mathbf{r} - \mathbf{R}') \Phi_{\mathbf{k}}(\mathbf{r}' - \mathbf{R})], \quad (3)$$

where $\Phi_{\mathbf{k}}(\mathbf{r}) \propto \exp[-|\mathbf{r}|^2/(2\sigma_\tau^2) + i\mathbf{k} \cdot \mathbf{r}]$ and \mathcal{N} ensures proper normalization. Below, we consider only scenarios where the right-hand side wave packet is initially at rest ($\mathbf{k}' = 0$) while the left-hand side wave packet initially possesses a finite incoming crystal momentum centered at $\mathbf{k} = (0.3\pi/a, 0)$ (see the snapshot sequences in Figs. 2 and 3).

For a convenient but adequate set of parameters relevant to semiconducting nanodevices, we choose $t = 1$ eV, which corresponds to an effective band mass of $m^* = 0.763 m_e$ in units of free electron mass m_e , and

$a = 0.5$ nm for the lattice spacing. Since the channel lengths of nanodevices will reach only a few tens of nm in the near future, we further base the wave packet simulation on a lattice of size 48×16 nm² (corresponding to $L_x \times L_y = 96 \times 32$ lattice sites), representing a rather long channel to reduce finite size effects.

The typical time evolution of a wave packet pair in the presence of a moderate finite electric field $E = 0.4$ MV/cm and in the absence ($U = 0$) or presence ($U = 2.0$ eV) of Coulomb interaction is summarized in Fig. 2, where $\sigma_r = 4.5$ nm. The snapshots in Figs. 2(a) and 2(c) for $U = 0$, which display the electron density $\rho(\mathbf{r}; \tau) = 2 \sum_{\mathbf{r}'} |\Psi(\mathbf{r}, \mathbf{r}'; \tau)|^2$ and the corresponding one-dimensional electron densities $\rho_x(x; \tau) = \sum_y \rho(\mathbf{r}; \tau)$ and $\rho_y(y; \tau) = \sum_x \rho(\mathbf{r}; \tau)$ [$\mathbf{r} = (x, y)$] along the x- and y-directions, respectively, clearly imply that the evolution of the wave packets is strongly determined by the lateral confinement in the y-direction and to a lesser extent by the Pauli exclusion principle (since we are considering spinless electrons only). Due to the confinement in the y-direction, the spreading of the wave packets and the subsequent reflection at the channel walls lead to interference along y, e.g., causing a pronounced temporary maximum on the channel centre line at $\tau = 16.46$ fs. The partial reflection of the incoming wave packet off the initially static wave packet due to Pauli exclusion also causes an, albeit much weaker, interference pattern along the x-direction. Most of the incoming wave packet, however, passes by the initially static wave packet such that both wave packets remain essentially distinct and intact, propagating with different and increasing velocities. Under the present electric field, the peak-to-peak amplitude of the corresponding Bloch oscillation amounts to $2s_0 = 4t/(eE) = 100$ nm, which substantially exceeds the channel length. [21]

The effect of finite Coulomb repulsion ($U = 2$ eV) is clearly visible in the snapshot sequences of Figs. 2(b) and 2(d). Due to the Coulomb interaction, the incoming wave packet pushes the initially resting wave packet forward and enhances the transverse expansion along the y-direction. The latter results in a more pronounced interference pattern along y, with the overall probability weight of the wave packets pushed further toward the channel edges. The Coulomb interaction also slightly enhances the charge transport along the longitudinal channel direction, as can be seen from the total charge transported across the line at $x_0 = 23.5$ nm [see Fig. 2(e)]. The total transported charge $Q(\tau)$ can be obtained by integrating the probability current density in the x-direction over time and the channel width. The x-component of the current density operator is given by

$$j^x(\mathbf{r}; \tau) = -\frac{ita}{\hbar} [e^{-i\frac{ie}{\hbar}Ea\tau} c_{\mathbf{r}-\mathbf{a}_x}^\dagger c_{\mathbf{r}} - \text{h.c.}], \quad (4)$$

which can be derived from the appropriate continuity

equation, [22] yielding

$$Q(\tau) = (-e) \sum_y \int_0^\tau \langle \psi(\tau') | j^x(x_0, y; \tau') | \psi(\tau') \rangle d\tau'. \quad (5)$$

Furthermore, we note that the time dependence of the total transported charge seems largely independent of the initial size, shape (e.g., quasi-one-dimensional Gaussians versus circular Gaussians) or positions (centered or slightly off-centered with respect to each other) of the wave packets. Finally, the interaction strength $U = 2t$ used here seems large, but was chosen to highlight the qualitative impact of Coulomb repulsion on the wave packet evolution, which we found is qualitatively similar for $U = t, 2t, 3t$ ($= 1, 2, 3$ eV).

The effect of a moderate electric field in the presence of finite Coulomb repulsion ($U = 2.0$ eV) is displayed in Fig. 3, which compares the wave packet evolution for $E = 0$ and 0.4 MV/cm. Here, we have chosen a pair of initially smaller wave packets with $\sigma_r = 1.5$ nm, which spread more quickly with time and generate a more heavily modulated density distribution in the transverse channel direction [cf. panels (c) and (d) of Figs. 2 and 3]. The wave function nevertheless maintains a larger weight near the channel edges than in the centre, similar to the findings above.

More strikingly, however, the overall expansion of the electron density in the x-direction is drastically reduced in the presence of a finite electric field [cf. the snapshots in Figs. 3(a)-3(d) at time $\tau = 26.33$ fs], where a density maximum in the x-direction clearly develops within the simulation period. A similar electric field effect can also be observed in the case of larger initial wave packets. The electric field, expectedly, also leads to a significant increase in the transported charge [Fig. 3(e)]. In the absence of an external field, the transported charge starts to saturate near unit charge $|e|$ at about $\tau = 20$ fs, indicating that, despite the (weakly) current enhancing influence of the Coulomb interaction, largely only one electron wave packet reaches the right half of the channel during the simulation time.

By modeling the initial electron probability distribution via two interacting wave packets, the present study takes a semiclassical approach to charge transport in a planar nanochannel. [9, 10] Our simulations show that the uniform spreading of the wave packets is limited along the transverse channel direction due to both interference effects and Coulomb repulsion. As a result, the electron density is strongly modulated along the y-direction, exhibiting a stationary statelike distribution. However, it propagates along the channel x-direction with a relatively large probability weight near (but not too close to) the channel edges. This density pattern can also be interpreted as the pair of electrons occupying only the low-lying transverse eigenmodes whose probability distribution is modified and pushed closer to the channel edges due to the Coulomb interaction. The details and

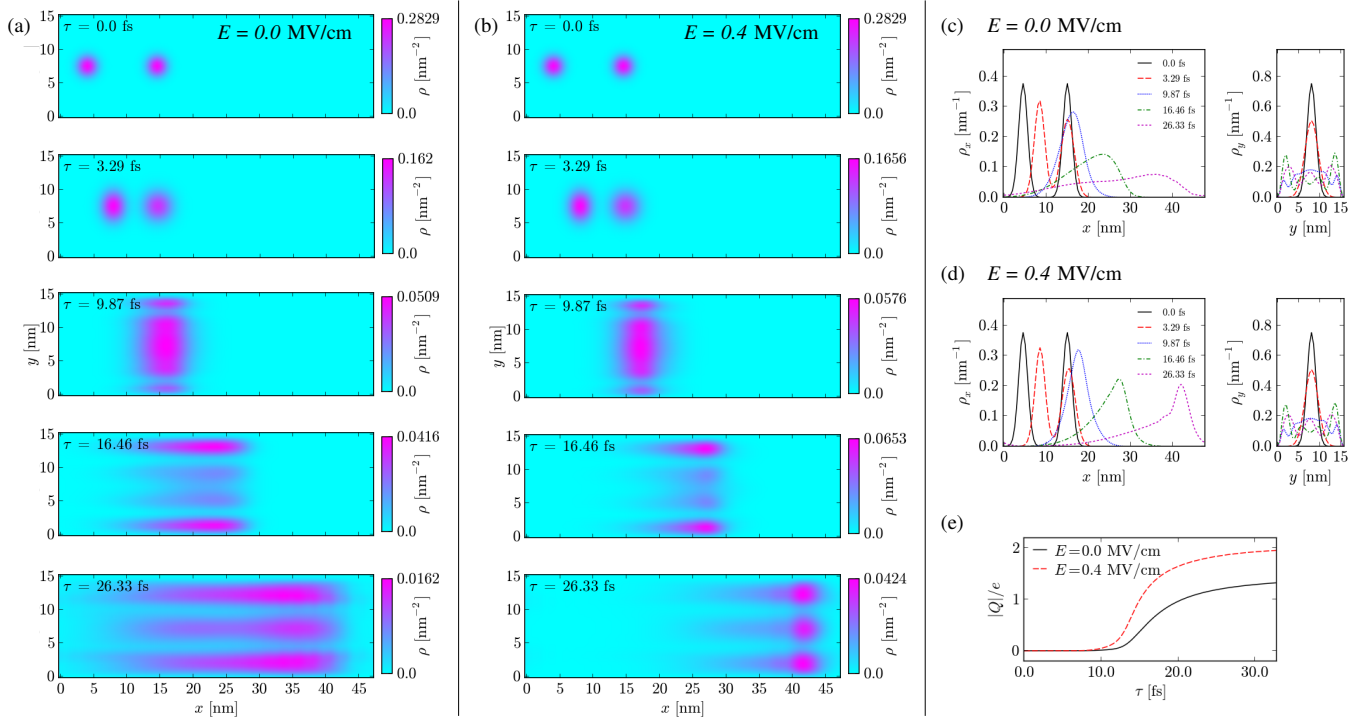


FIG. 3. Effect of an electric field applied in x-direction for a fixed Coulomb repulsion magnitude. (a), (b) Snapshots of the electron density $\rho(\mathbf{r}; \tau)$ for $E = 0$ and 0.4 MV/cm, respectively. (c), (d) Corresponding partially integrated one-dimensional electron densities $\rho_x(x; \tau)$ and $\rho_y(y; \tau)$ for $E = 0$ and 0.4 MV/cm, respectively. (e) Total charge transported across the half-way line at $x_0 = 23.5$ nm as a function of time τ . The initial wave packet sizes are given by $\sigma_\tau = 3a = 1.5$ nm, while $U = 2.0$ eV; only the initially left-hand side wave packet is initially given a finite momentum $\mathbf{k} = (0.3\pi/a, 0)$.

extent of such edge-dominated transport can have significant implications for the performance of nanodevices, where interface roughness and charge trapping at interfaces are known to lead to a substantial degradation of the electron mobility. [4, 5]

Furthermore, we find that for typical nanochannel length and time scales, an electric field has a stabilizing effect on electron wave packets, inhibiting spreading along the channel direction. This behavior reinforces the more particle-like picture of electrons in a nanochannel, lending support to particle-based classical or semiclassical studies such as classical Monte Carlo and/or molecular dynamics methods to solve the classical Boltzmann transport equation in the presence of interactions and impurities. The stabilizing effect of an electric field has also been observed for strictly one-dimensional interacting wave packets based on a time-dependent Hartree-Fock approach, which additionally revealed a bunching phenomenon of wave packets within the one-dimensional channel. [11]

In conclusion, we have considered the effect of Coulomb repulsion and external field on the electron dynamics in a nanochannel, by exactly solving the Schroedinger equation for a pair of interacting and propagating electrons. This is in contrast to previous wave packet studies that mostly focused on single electrons and/or one-

dimensional nanostructures. [12–16] The present wave packet simulation may be extended in future studies to include, e.g., the electronic spin degree of freedom, small three-dimensional nanostructures, more than two interacting electrons and, though more challenging, the coupling to high-density source and drain contacts.

The authors thank Y. Tokura for useful discussions.

* cpuetter@comas.frsc.tsukuba.ac.jp

- [1] *ITRS 2011 Edition*, p. 10, Table PIDS2.
- [2] N. Sano: *Jpn. J. Appl. Phys.* **50** (2011) 010108.
- [3] N. Sano: *J. Comput. Electron.* **10** (2011) 98.
- [4] T. Kamioka, H. Imai, Y. Kamakura, K. Ohmori, K. Shiraishi, M. Niwa, K. Yamada, and T. Watanabe: *IEDM Tech. Dig.*, 2012, p. 17.2.1.
- [5] W. Feng, R. Hettiarachchi, Y. Lee, S. Sato, K. Kakushima, M. Sato, K. Fukuda, M. Niwa, K. Yamabe, K. Shiraishi, H. Iwai, and K. Ohmori: *IEDM Tech. Dig.*, 2011, p. 27.7.1.
- [6] C.-W. Lee, A. Afzalian, N. D. Akhavan, R. Yan, I. Ferain, and J.-P. Colinge: *Appl. Phys. Lett.* **94** (2009) 052511.
- [7] S. Datta: *Quantum Transport: Atom to Transistor* (Cambridge University Press, Cambridge, 2005).
- [8] H. Haug and A.-P. Jauho: *Quantum Kinetics in Transport and Optics of Semiconductors* (Springer-Verlag,

- Berlin, 2010) 2nd ed.
- [9] D. Xiao, M.-C. Chang, and Q. Niu: *Rev. Mod. Phys.* **82** (2010) 1959.
 - [10] R. Shindou and K.-I. Imura: *Nucl. Phys. B* **720** (2005) 399.
 - [11] T. Shiokawa, G. Fujita, Y. Takada, S. Konabe, M. Muraguchi, T. Yamamoto, T. Endoh, Y. Hatsugai, and K. Shiraishi: *Jpn. J. Appl. Phys.* **52** (2013) 04CJ06.
 - [12] F. Claro, J. F. Weisz, and S. Curilef: *Phys. Rev. B* **67** (2003) 193101.
 - [13] Y. Fu and M. Willander: *J. Appl. Phys.* **97** (2003) 094311.
 - [14] W. S. Dias, E. M. Nascimento, M. L. Lyra, and F. A. B. F. de Moura: *Phys. Rev. B* **76** (2007) 155124.
 - [15] J. M. Pruneda and I. Souza: *Phys. Rev. B* **79** (2009) 045127.
 - [16] T. Kramer, C. Kreisbeck, and V. Krueckl: *Phys. Scr.* **82** (2010) 038101.
 - [17] J. S. de Sousa, L. Covaci, F. M. Peeters, and G. A. Farias: *J. Appl. Phys.* **112** (2012) 093705.
 - [18] M. Suzuki: *Phys. Lett. A* **146** (1990) 319.
 - [19] M. Suzuki: *J. Phys. Soc. Jpn.* **61** (1992) 3015.
 - [20] Y. Hatsugai and A. Sugi: *Int. J. Mod. Phys. B* **15** (2001) 2045.
 - [21] T. Hartmann, F. Keck, H. J. Korsch, and S. Mossmann: *New J. Phys.* **6** (2004) 2.
 - [22] D. R. da Costa, A. Chaves, G. A. Farias, L. Covaci, and F. M. Peeters: *Phys. Rev. B* **86** (2012) 115434.